Pergamon

0038-1101(94)00162-6

Solid-State Electronics Vol. 38, No. 3, pp. 715–720, 1995
Copyright © 1995 Elsevier Science Ltd
Printed in Great Britain. All rights reserved
0038-1101/95 $9.50 + 0.00

LATERAL TITANIUM SILICIDE GROWTH AND ITS SUPPRESSION USING THE a-Si/Ti BILAYER STRUCTURE

YUNG-SONG LOU and CHING-YUAN WU†

Advanced Semiconductor Device Research Laboratory and Institute of Electronics, National Chiao-Tung University, Hsin-Chu, Taiwan, R.O. China

(Received 21 March 1993; in revised form 14 July 1994)

Abstract—The effects of internal oxygen impurities released from the Ti–SiO_2 reaction on the lateral silicide growth using the a-Si/Ti bilayer structure are presented. The lateral silicide growth can be effectively retarded by internal oxygen impurities using a-Si/Ti bilayer process after silicidation at a temperature below 700°C. Compared with the simultaneously processed single Ti layer process, it is observed that both high-level oxygen impurities and their redistribution in the possible Si diffusion paths play the same important role on the suppression of the lateral silicide growth. Finally, the oxygen-redistribution-dependent kinetics is developed to give a self-consistent explanation for the experimental observations from both the single Ti layer process and the a-Si/Ti bilayer process.

1. INTRODUCTION

Recently, the self-aligned silicidation (SALICIDE) technology has been extensively studied because of its important application in MOS/VLSI fabrication as MOS devices are scaled down to submicron dimension[1]. Among all refractory silicides, $TiSi_2$ is the most promising material for this technology due to its low resistivity and high thermal stability[2]. Since silicon atoms are the dominant diffusion species during thermal reaction, the out-diffusion of Si atoms will lead to the lateral silicide formation over the sidewall oxide spacers and further results in short-circuit between the gate and the source/drain. This undesirable bridging phenomenon has been minimized by several techniques[3–7]. Among them, the reaction performed in a purified nitrogen ambient has been widely used to prevent Si movement during the $TiSi_2$ process. Because of the formation of titanium nitride over the oxide region, the lateral silicide growth is consequently inhibited[3]. The NH_3 plasma-assisted thermal annealing has also been developed to enhance the surface nitridation of titanium during silicidation[4]. However, the competing formation of $TiSi_2$ and TiN on the Si region cannot be avoided, resulting in the uneven loss of Ti metal and further making the precise control of Ti silicidation impossible. Since the shortest possible time at a fixed temperature can be provided to reduce the chance of bridging, the rapid thermal annealing (RTA) instead of the conventional furnace annealing has been explored[5]. Although the critical process temperature and time have been proposed to suppress the lateral silicide growth, it is still impossible to completely convert Ti metal into $TiSi_2$ without the lateral silicide growth. Also, the influence of the ambient gas on the silicide formation and the lateral silicide growth still exists. Recently, the extent of lateral Si diffusion has been greatly suppressed by using ion implantation through Ti metal film[6]. With the subsequent RTA process, not only the retardation of lateral silicide growth can be achieved, but also a shallow junction can be obtained[7]. Although the silicide reaction rate can be enhanced by the dispersion of the interfacial oxide barrier, the ion-beam-induced mixing of Ti and SiO_2 and the associated chemical effects still need further investigation for application in VLSI devices[8]. Moreover, the degradation of gate-spacer isolation integrity has been shown to strongly depend on whether Si ion mixing is used in the Ti SALICIDE process. It is found that Si ion implantation through Ti metal will result in the enhanced deeper Ti penetration into SiO_2 and the formation of a Ti-rich oxide layer to generate a leakage path[9].

In this paper, a simple method using the a-Si/Ti bilayer metallization[10,11] is proposed to suppress the lateral silicide growth. After silicidation at a temperature below 700°C, the lateral diffusion of Si atoms is found to be inhibited by the oxygen impurities released from the internal reaction between Ti and SiO_2. Then, by comparing with that of single Ti layer on the patterned poly-Si island, the lateral-growth-free and self-aligned features are demonstrated by Scanning Electron Microscopy (SEM). Moreover, a test structure with a thin W interposing layer selectively deposited over the SiO_2 region to mask the Ti–SiO_2 reaction is designed to identify the proposed oxygen-dependent lateral growth mechanism. Finally, the oxygen-redistribution-related kinetics is proposed to give a self-consistent interpretation of the lateral

†To whom all correspondence should be addressed.

silicide growth for both the single Ti layer process and the a-Si/Ti bilayer process.

2. EXPERIMENTAL PROCEDURE

The (100), 5–15 Ω · cm, *n*-type Si wafers with or without thermally grown SiO_2 were used as the substrates. The poly-Si film of 4000 Å was deposited on the oxidized substrate by a LPCVD reactor and doped by $POCl_3$ source and then patterned by plasma etching. The positive photoresist was used to define the poly-Si island. The patterned samples were used to monitor the lateral silicide growth during thermal annealing. For part of the patterned poly-Si samples, the positive photoresist over the poly-Si surface was preserved as a self-aligned lift-off mask for selective deposition of W layer (100 Å) on the exposed SiO_2 region. Since the reaction between Ti and SiO_2 will be retarded by the thin W layer, the effect of the Ti–SiO_2 reaction on the lateral silicide growth can be evaluated by using these specially designed test structures. After a standard cleaning process, the substrates were immediately etched in a dilute HF solution (HF : H_2O = 1:15) prior to loading into the vacuum system. Since the strength of HF is diluted and the dip time is short, the thin W layer can be retained after etching in the HF solution. The thin titanium film was deposited by an E-gun evaporator with a base pressure of about 5×10^{-6} torr, then the a-Si film was evaporated subsequently without breaking the vacuum[10,11]. For the most cases, the samples with a-Si capping were annealed in N_2 ambient at a temperature varied from 400 to 900°C for 5–120 min, and there was not any special equipment used to minimize the oxygen content within N_2 before introducing to the furnace. For comparisons, both the single Ti layer and the a-Si/Ti bilayer on the patterned poly-Si island were simultaneously annealed in Ar ambient to investigate the effects of a-Si capping on the lateral silicide formation. It should be noted that a special furnace is designed to reduce the oxygen content in Ar ambient by a preheated Ti sponge filter and thus to prevent the single Ti layer from oxidation. The lateral silicide growth was evaluated by SEM after 650°C annealing and selective etching in $NH_4OH + H_2O_2 + 4H_2O$ (NHH) solution at 50–60°C.

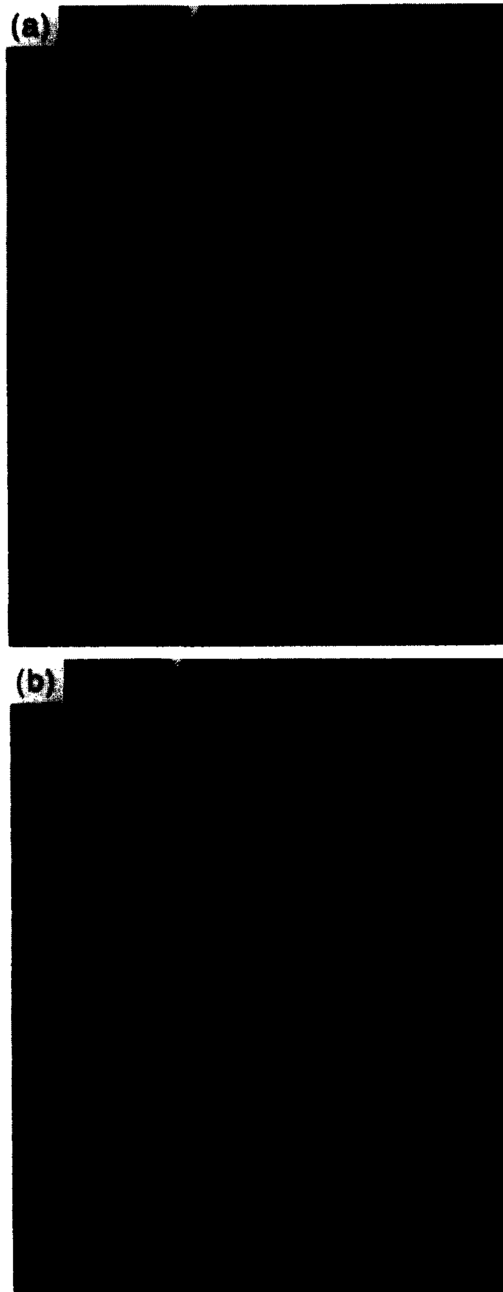

Fig. 1. The SEM microphotographs of (a) 90 Å a-Si/1000 Å Ti bilayer, and (b) the single Ti layer of 1000 Å.

3. RESULTS AND DISCUSSIONS

For the SALICIDE technology, the control of lateral silicide growth during the initial sintering step is the most important consideration. The lateral silicide growth and the self-aligned growth of $TiSi_2$ are carefully examined using the SEM microphotographs for both the single Ti layer and the a-Si/Ti bilayer on the patterned poly-Si island after simultaneously annealing at 650°C in Ar ambient for 30 min and the selective etching in solution. For the SEM microphotographs shown in Fig. 1(a), a well-defined edge between the grown $TiSi_2$ region and the SiO_2 substrate without any residue left on the exposed SiO_2 surface is observed for the case of 90 Å a-Si/1000 Å Ti bilayer. On the contrary, the significant lateral silicide growth with 1.3 μm beyond the patterned poly-Si edges is clearly demonstrated for the case of the single Ti layer of 1000 Å, as shown in Fig. 1(b). In order to explain the difference in the experimental observations, the dependence of lateral silicide growth on the Ti–SiO_2 reaction is evaluated. Figures 2(a) and 3(a) show the SEM microphotographs of the simultaneously processed a-Si/Ti bilayer and single Ti layer on the poly-Si island after 700°C

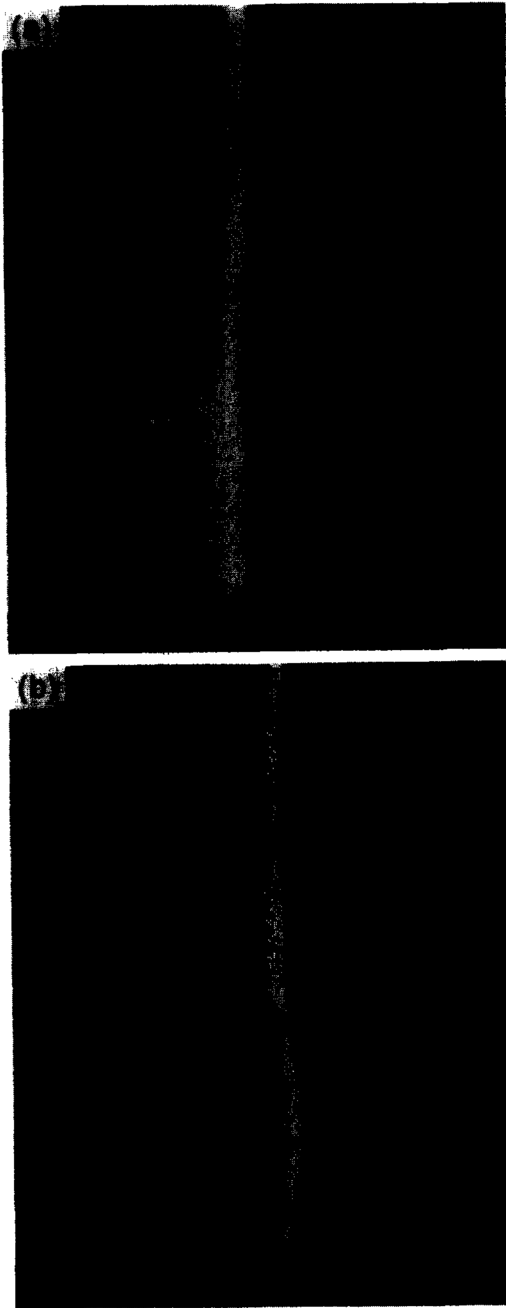

Fig. 2. The SEM microphotographs for the 90 Å a-Si/1000 Å Ti bilayer on the patterned poly-Si island (a) without, and (b) with a thin W layer over SiO_2 after 700°C annealing in Ar ambient for 60 min.

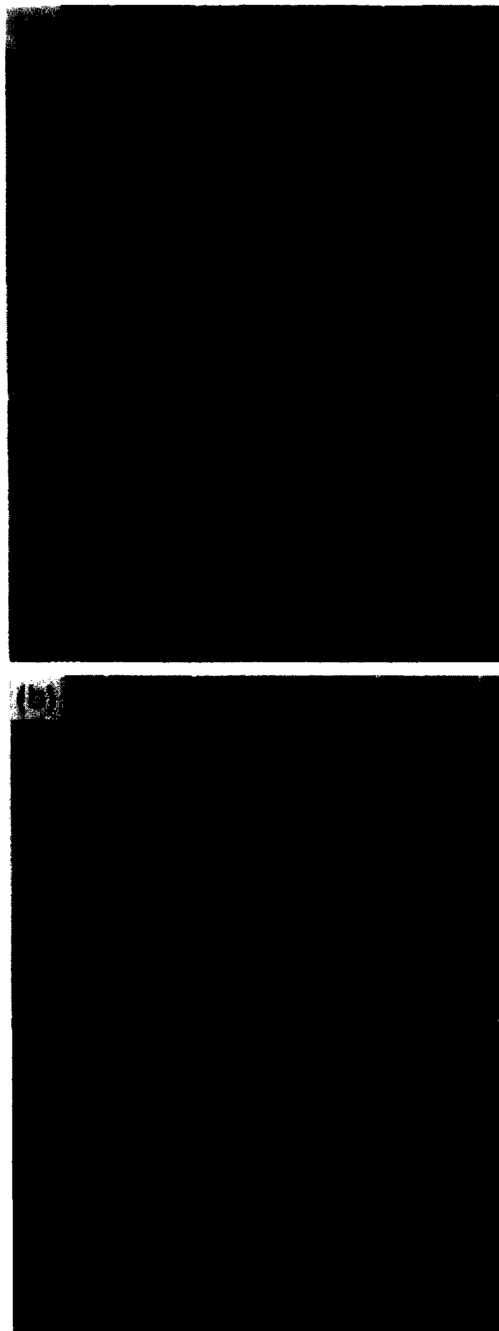

Fig. 3. The SEM microphotographs for the single Ti layer of 1000 Å on the patterned poly-Si island (a) without, and (b) with a thin W layer over SiO_2 after 700°C annealing in Ar ambient for 60 min.

annealing in Ar ambient for 60 min, respectively. Similar to that of 650°C annealing, the obvious lateral silicide growth with more than 3 μm is found only for the single Ti layer case. The SEM microphotographs for the a-Si/Ti bilayer and the single Ti layer on a specially designed test structure with the Ti–SiO_2 reaction inhibited by the selectively deposited W layer of 100 Å over the SiO_2 surface are shown in Fig. 2(a) and (b), respectively. It is interesting to note that once the interaction between Ti and SiO_2 is isolated by the thin W interposing layer, the lateral growth can occur and reach $\sim$1.2 μm for the a-Si/Ti bilayer case, as shown in Fig. 2(b). Compared with Fig. 2(a) in which the Ti–SiO_2 reaction is proceeded during thermal reaction, it reveals that the incorporation of oxygen impurities released from the reduction of SiO_2 by Ti into the interface Ti_5Si_3 layer and the unreacted Ti metal is the major mechanism for the

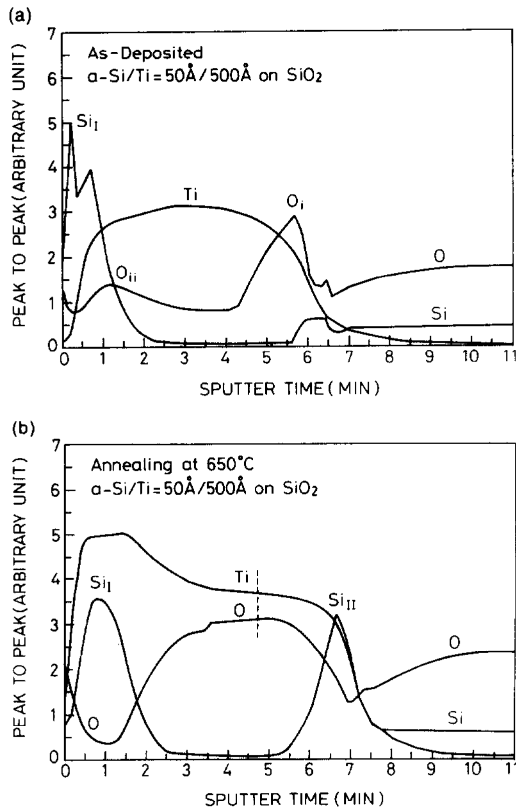

Fig. 4. The AES depth profiles of 50 Å a-Si/500 Å Ti bilayer structure on SiO_2 (a) as-deposited, and (b) after 650°C annealing in N_2 ambient.

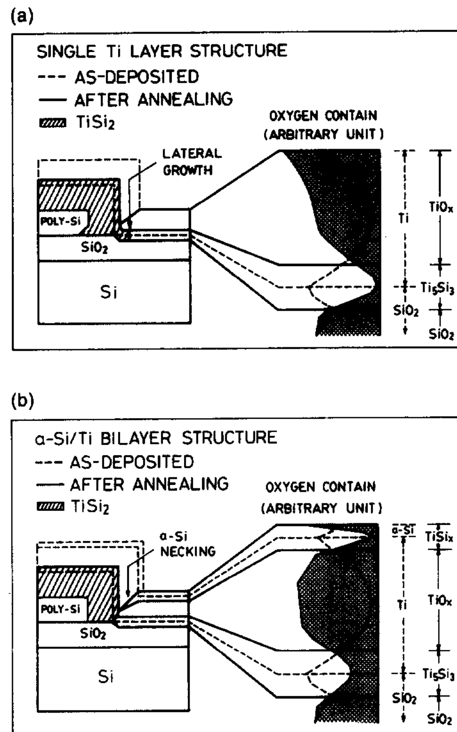

Fig. 5. The schematic diagram of the relative oxygen depth profiles within the as-deposited metal and the resulted products on SiO_2 after thermal annealing at 650°C for (a) the single Ti layer, and (b) the a-Si/Ti bilayer structures. The corresponding layer structure on the patterned poly-Si island is also described.

suppression of the lateral out-diffusion of Si atoms. However, the serious lateral silicide growth still appears for the single Ti layer case although the amount of oxide loss is compatible for both the single Ti layer and the a-Si/Ti bilayer cases as obtained for the samples with different Ti thicknesses after simultaneously annealing at different sintering temperatures. This implies that the ambient effect, which is probably due to the interaction between the residual oxygen impurities in the annealing ambient and the Ti metal, cannot be neglected. The acceptable interpretation for these results is that the redistribution of released oxygen impurities plays an essential role for the lateral silicide formation.

The AES depth profile of the as-deposited 50 Å a-Si/500 Å Ti bilayer on SiO_2 is shown in Fig. 4(a). By comparing the AES depth profile of the as-deposited sample with that of the sample annealed at 650°C, it reveals that not only a sharp Si peak named as Si_{II} appears at the Ti/SiO_2 interface but also the oxygen profile is drastically redistributed as shown in Fig. 4(b). Many investigations[5,12–14] have found that Ti would start to react with SiO_2 after annealing above 500°C. Accordingly, the chemical reaction between Ti and SiO_2 can be expressed as:

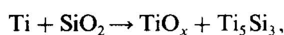

$$Ti + SiO_2 \rightarrow TiO_x + Ti_5Si_3,$$

with the thin metal-rich silicide layer distinctly sandwiched between the top metal oxide layer and the bottom SiO_2 substrate.

It is interesting to study the effect of the interaction between a-Si and Ti on the redistribution of oxygen impurities within the unreacted metal over the SiO_2 region. From Fig. 4(b), it is clearly seen that the disappearance of the oxygen peak O_{ii} originally existed at the a-Si/Ti interface as shown in Fig. 4(a) can be attributed to the a-Si–Ti reaction because the annealing temperature for a-Si to react with Ti can be as low as 525°C[15]. For the moderate thickness of a-Si film on Ti metal, the selective etching behavior can be maintained since the resulted products over the surface is metal-rich silicide layer which can be easily etched off by the conventional wet etching method. If we compare the arbitrary level of oxygen impurities in the surface metal-rich silicide layer with that in the bottom Ti_5Si_3 layer, a comparatively large amount of oxygen content is found to be embedded within the bottom Ti_5Si_3 layer and is independent of the as-deposited Ti thickness, as shown in Fig. 4(b) and Fig. 5(a, b). More attention should be paid to explain this observation. From the previous investigations using Rutherford Backscattering Spectrometry (RBS) [12], AES depth profile[5], and Elastic Recoil Detection (ERD)[14], the interface Ti_5Si_3 layer contains only a small amount of oxygen impurities for the single Ti layer process. In this process, the interaction between

Ti and residual oxygen impurities contaminated in the annealing ambient is hardly avoided because of the high chemical reactivity nature of Ti metal. Such an interaction will act as a sink for internal oxygen impurities and leads to a lower concentration of oxygen impurities at the TiO_x/SiO_2 interface. It should be noted that the concentration of external oxygen impurities considered in this situation is assumed to be smaller than a critical level in order to prevent severe degradation of the formed $TiSi_2$ film or oxidation of Ti metal on SiO_2. On the other hand, the oxidation of Ti metal is prevented by the thin a-Si capping layer and a new metal-rich silicide layer is developed over the surface region for the a-Si/Ti bilayer process. The interaction between a-Si and Ti is assumed to induce a driving force to deplete the oxygen impurities out of the surface region, thus the interface Ti_5Si_3 layer is embedded with oxygen impurities. It is therefore reasonable to expect that the resulted surface products due to the interaction between oxygen-contaminated ambient and Ti metal for the single Ti layer process or a-Si and Ti for the a-Si/Ti bilayer process will induce different oxygen profiles and thus results in different reactions for the lateral silicide formation.

Another interesting aspect, which can be deduced from the SEM observations, is that the driving force induced from the a-Si–Ti reaction has a strong effect on the lateral silicide formation. Comparing the lateral silicide growth of $\sim 1.25\,\mu m$ in Fig. 2(b) for the a-Si/Ti bilayer case with that shorting the lines in Fig. 3(b) for the single Ti layer case after eliminating the Ti–SiO_2 reaction by a thin W interlayer, it can be concluded that the a-Si–Ti reaction is also a necessary factor contributing to the feature of lateral-growth-free in addition to the oxygen impurities released from Ti–SiO_2 reaction for the a-Si/Ti bilayer process. Moreover, the more serious lateral growth of $>7\,\mu m$ after masking the Ti–SiO_2 reaction as shown in Fig. 3(b) compared with that of $\sim 3\,\mu m$ with normally proceeded Ti–SiO_2 reaction as shown in Fig. 3(a) reveals that the effect of oxygen impurities on the lateral silicide growth cannot be neglected even in the single Ti layer process. Although the activation energy for the lateral silicide growth is obtained to be about 1.89 eV after annealing above 750°C[16], we believe that the real activation energy for the lateral silicide growth can be further reduced if the internal oxygen barrier effect can be avoided.

In the past, the most common explanation for the lateral silicide formation is the diffusion of Si atoms through the silicide layer laterally into the conformal metal film over the SiO_2 region if Si is the dominant diffuser during thermal silicidation, e.g. refractory metals and noble metals at high temperatures. However, this explanation does not consider the effect of internal oxygen impurities on the out-diffusion of Si flux. By considering the Ti–SiO_2 reaction and the redistribution of internal oxygen impurities, the observed lateral silicide growth for the single Ti layer process may result from the lateral diffusion of Si atoms through the interface Ti_5Si_3 layer. A small amount of oxygen content within the Ti_5Si_3 layer may be due to the interaction between Ti and external oxygen impurities, which enhances the out-diffusion of internal oxygen impurities. The schematic diagram showing the relative depth profiles of oxygen impurities within both the as-deposited metal film and the resulted products on SiO_2 after thermal annealing are shown in Fig. 5(a). The lateral silicide growth along the interface Ti_5Si_3 layer is also shown for more detailed visualization.

We may conclude that the lateral diffusion of Si atoms is inhibited in the a-Si/Ti bilayer process since the possible diffusion paths for Si atoms including the unreacted metal and the interface Ti_5Si_3 layer are all saturated by internal oxygen impurities from the Ti–SiO_2 reaction. The driving force to deplete the oxygen impurities out of the surface region and thus to stuff the diffusion path of the Ti_5Si_3 layer is believed to be due to the silicidation stress induced from the a-Si–metal reaction. Figure 5(b) shows the schematic diagram of the arbitrary oxygen depth profiles before and after thermal annealing. The relative oxygen intensity within the interface Ti_5Si_3 layer is clearly higher than that found in Fig. 5(a). It is interesting to study whether the surface silicide layer due to the a-Si–Ti reaction is a possible conduction path for Si atoms because only a small amount of oxygen impurities exists within this layer. Considering the volume reduction after silicidation on the poly-Si region and the competing reactions of Ti–SiO_2 and Ti–poly-Si at the boundary between poly-Si and SiO_2, the corresponding reaction products on the pattern poly-Si island after thermal annealing can be described by the layer structure, as shown in Fig. 5(b). During thermal annealing, the large volume reduction of metal film on the poly-Si region is expected to be due to the consumption of Si atoms by the silicide formation. However, the final thickness of the resulted products over the SiO_2 region is nearly unchanged due to the relatively weak reactions of a-Si–Ti and Ti–SiO_2 as compared with that of Ti–poly-Si. As a result, a serious necking effect for the a-Si film along the $TiSi_2/TiO_x$ boundary is observed. Thus, the necking effect of a-Si film will make the lateral diffusion of Si atoms through the surface channel impossible. Such a conclusion coincides well with our SEM observations.

The dependence of the lateral silicide growth on internal oxygen impurities and external oxygen impurities requires more detailed evaluations. In the single Ti layer process, it suffers from external oxygen impurities even in a tightly controlled environment because the trace amount of oxygen impurities can severely react with the exposed Ti metal to degrade the quality of the silicide film and results in the nonreproducible and nonuniform problems. It is not amazing to find that serious lateral silicide growth occurs in an oxygen-contained N_2 ambient using

RTA[7], while the contradictory result is obtained[3]. In [3], it is reported that the presence of O_2 in He ambient will inhibit the lateral extent of the reaction. A possible explanation for these observations based on our proposed reaction model may be due to different levels of oxygen content within the interface Ti_5Si_3 layer through the difference in ambient purity and annealing system, e.g. RTA or conventional furnace annealing. Perhaps, the previous interpretations for the lateral silicide growth are limited by the uncontrollable nature of the reaction between Ti metal and external oxygen impurities, thus the internal oxygen effect is always neglected for the single Ti layer process. However, using a thin a-Si film as a protective layer over the Ti metal layer, the external oxygen effect can be effectively isolated. At the same time, the retardation of the lateral silicide growth by internal oxygen impurities can be revealed.

4. CONCLUSIONS

After isolation of external oxygen impurities originally contaminated in the annealing ambient by the surface a-Si protective layer, the effect of internal oxygen impurities released from the reduction of SiO_2 by Ti on the lateral silicide growth is revealed. Moreover, the saturation of the unreacted metal and the interface Ti_5Si_3 layer by internal oxygen impurities is responsible for the suppression of the lateral silicide growth and the termination of the Ti–SiO_2 reaction. By considering the surface interaction and their effects on oxygen redistribution, a self-consistent reaction model is proposed to explain the difference in the observed SEM results of the lateral silicide growth for both the single Ti layer process and the a-Si/Ti bilayer process. The major features of this study are not only to give the general nature of the proposed model for different thin film systems with the reactive metal over the dielectric substrate during thermal silicidation but also to provide a simple method using the a-Si/Ti bilayer process for solving the lateral silicide growth problem.

Acknowledgement—The authors would like to express their sincere thanks to the National Science Council, Taiwan, Republic of China, for continuous grant support under the contract NSC-81-0404-E009-139.

REFERENCES

1. C. Y. Ting, *IEDM Tech. Dig.*, p. 110 (1984).
2. S. P. Murarka, *Silicides for VLSI Applications.* Academic Press, New York (1983).
3. S. S. Iyer, C. Y. Ting and P. M. Fryer, *J. Electrochem. Soc.* **132,** 2240 (1985).
4. B. Z. Li, S. F. Zhou, J. Li and T. A. Tang, *J. Vac. Sci. Technol.* **B5,** 1667 (1987).
5. L. J. Brillson, M. L. Slade, H. W. Richter, H. Vander Plas and R. T. Fulks, *Appl. Phys. Lett.* **47,** 1080 (1985).
6. L. R. Zheng, L. S. Hung, J. W. Mayer and K. W. Choi, *Nucl. Instr. Meth. Phys. Rev.* **B/7–8,** 413 (1985).
7. Y. H. Ku, S. K. Lee, D. K. Shih and D. L. Kwong, *Appl. Phys. Lett.* **52,** 877 (1988).
8. G. M. Mattinssi, *J. Vac. Sci. Technol.* **B4,** 1352 (1986).
9. J. J. Sung and C. Y. Lu, *IEEE Electron Device Lett.* **EDL-10,** 481 (1989).
10. H. H. Tseng and C. Y. Wu, *IEEE Electron Device Lett.* **EDL-7,** 623 (1986).
11. Y. S. Lou, H. C. Cheng and C. Y. Wu, *IEEE Trans. Electron Devices* **ED-39,** 1835 (1992).
12. C. Y. Ting, M. Wittmer, S. S. Iyer and S. B. Brodsky, *J. Electrochem. Soc.* **131,** 2934 (1984).
13. R. Pretorius, J. M. Harris and M. A. Nicolet, *Solid-St. Electron.* **21,** 667. (1978).
14. G. J. P. Krooshof, F. H. P. M. Habraken and W. F. Van der Weg, *J. appl. Phys.* **63,** 5110 (1988).
15. L. S. Hung, J. Gynla and J. W. Mayer, *J. appl. Phys.* **54,** 5076 (1983).
16. P. Revesz, J. Gyimesi, L. Pogany and G. Peto, *J. appl. Phys.* **54,** 2114 (1983).